

Sn-Filled Single-Crystalline Wurtzite-Type ZnS Nanotubes**

Junqing Hu, Yoshio Bando, Jinhua Zhan, and
Dmitri Golberg*

Since the discovery of carbon nanotubes,^[1] a large number of inorganic solids with layered or nonlayered crystal lattices have been found to form tubular nanostructures.^[2] Nowadays, inorganic nanotubes with interesting properties and potential applications constitute an important class of compounds. Among these, Group II–VI semiconductors (e.g., ZnS, ZnSe, CdS, CdSe) are particularly important, and great efforts have been made to fabricate their nanowires, nanorods, and nanoribbons (or nanobelts) by various routes^[3] because of their unique optical, electrical, and optoelectronic properties, and potential technological applications.^[4] Thus, new synthesis pathways for the formation to nanotubes of these materials are in demand; however, there have been only a few reports on the synthesis of their tubular structures. Rao et al.^[5] obtained CdS and CdSe nanotubes by surfactant-assisted synthesis, and these were the first examples of nanotubes made of the Group II–VI semiconductors. Xie and co-workers^[6] obtained CdS nanotubes by an in situ micelle–template–interface reaction. Recently, Wang et al.^[7] generated ZnS nanotubes by reaction of ZnO nanoribbons (as templates) with H₂S, and Zhu et al.^[8] obtained ZnS nanotubes by a high-temperature thermochemical process from ZnS powders. However, the CdS, CdSe, and ZnS nanotubes obtained in these cases are polycrystals, consisting of numerous nanocrystallites, rather than single crystals. This would negatively affect their semiconducting performance in real devices. The synthesis of single-crystalline nanotubes of the Group II–VI semiconductors has not been realized experimentally and still remains a challenge.

Among the many routes for synthesizing tubular structures of nonlayered materials, the template-based method offers a wide range of advantages.^[9] Recently, single-crystalline GaN and Si nanotubes were prepared by a template-based process,^[10] in which ZnO and ZnS nanowires, respectively, were used as one-dimensional removable templates. We assumed that using an analogous route and a suitable template could provide access to single-crystalline nanotubes of the Group II–VI semiconductors. Indeed we have succeeded in synthesizing single-crystalline wurtzite-type ZnS

[*] Dr. J. Hu, Prof. Y. Bando, Dr. J. Zhan, Dr. D. Golberg
Advanced Materials Laboratory
National Institute for Materials Science (NIMS)
Namiki 1-1, Tsukuba, Ibaraki 305-0044 (Japan)
Fax: (+81) 298-51-6280
E-mail: hu.junqing@nims.go.jp

[**] This work was supported by the Japan Society for the Promotion of Science (JSPS) Fellowship tenable at the National Institute for Materials Science, Tsukuba, Japan.

nanotubes for the first time by a novel Sn-nanorod-templated process.

The ZnS nanotubes were synthesized in a horizontal high-temperature resistance furnace at a temperature of 1150 °C by using a mixture of ZnS and SnO powders as starting materials. After the furnace was cooled to room temperature under a stream of N₂, a gray-colored product was collected from the inner wall of the tube downstream, where the temperature was between 180 and 250 °C during heating. As shown in the scanning electron microscopy (SEM) image (Figure 1 a),

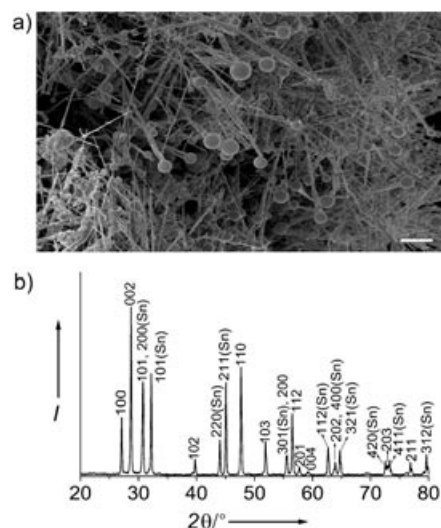


Figure 1. a) SEM image of as-grown ZnS nanostructures. Scale bar: 1 μm. b) XRD spectrum of the product.

numerous one-dimensional nanostructures with spherical particles at their tip ends were formed in the product. Most of them are straight and have lengths ranging from several to tens of micrometers. The X-ray diffraction (XRD) pattern (Figure 1 b) of the product presents clear evidence that the nanostructures are composed of two crystalline phases, that is, hexagonal (wurtzite) ZnS (JCPDS: 36-1450; $a = 3.8298$ Å and $c = 6.2573$ Å) and tetragonal Sn (β-Sn) (JCPDS: 04-0673; $a = 5.831$ Å and $c = 3.182$ Å). No characteristic peaks from other impurities, such as ZnO, SnO, and SnO₂ are detected in the XRD pattern.

Transmission electron microscopy (TEM) and X-ray energy-dispersive spectrometry (EDS) reveal that the as-grown structures are in fact ZnS nanotubes filled with Sn. Normally, a Sn-filling occupies more than 70–80% of the entire cavity of a ZnS nanotube. Some of tubes have uniform diameters and wall thicknesses throughout their whole lengths (Figure 2 a), and the diameters and wall thicknesses are 150–200 nm and 50–60 nm, respectively. Typically, a given tube is sealed with a Sn-filling at one end (note that each Sn-filling terminates with a spherical Sn particle), whereas the other end and central part of the tube may be open and hollow, respectively. As shown in Figure 2 b, the diameters and wall thicknesses of these tubes gradually decrease and become smaller and smaller along their lengths, from 180–250 nm and 60–80 nm at the thicker end to 80–120 nm and 25–

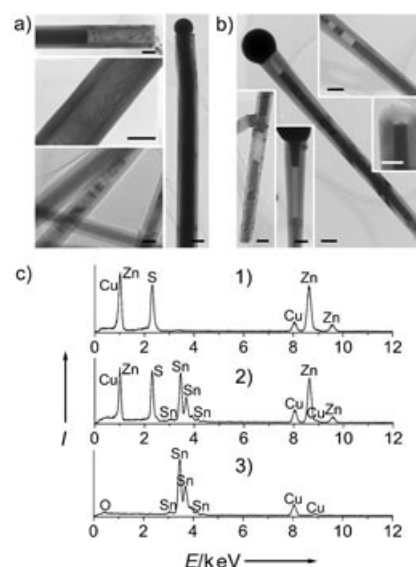


Figure 2. Typical TEM images showing the filling characteristics of Sn inside the ZnS nanotubes. a) ZnS nanotubes with the uniform diameters throughout the whole length. b) ZnS nanotubes for which the diameters gradually decrease along the length. The middle-right inset shows the cross-sectional shape at one end of a Sn-filled ZnS nanotube. Scale bars: 100 nm. c) Energy-dispersive spectra recorded for a tubular sheath or a tube cavity (curve 1), a filling (curve 2), and a spherical Sn particle (3, shown in b) on the end of the tube.

50 nm at the thinner end. Usually, a large spherical Sn particle (several hundred nanometers in diameter) seals the thicker end, and the thinner end is filled with a Sn nanorod, whereas the middle section is a hollow tubular cavity. In some cases, the Sn-fillings divide a tube into independent hollow segments, otherwise the Sn-fillings spread through the entire length, forming a continuous Sn-cored and ZnS-shelled core/shell structure. A quasi-circular cross-sectional shape can easily be viewed at one end of a Sn-filled ZnS nanotube (middle-right inset TEM image, Figure 2 b), suggesting that the ZnS nanotube is not a faceted tube, but rather a cylindrical (or taper-like) tube. The energy-dispersive spectra shown in Figure 2 c were recorded for a tubular sheath or a tube cavity (curve 1), a Sn-filling (curve 2), and a Sn particle (curve 3) attached to the end of a tube, confirming that the wall has the chemical composition of ZnS, and the filling is metallic Sn.

High-resolution TEM imaging and electron diffraction reveal that all as-grown ZnS nanotubes are structurally uniform single crystals. Figure 3 a is an image taken from a tube wall with a uniform thickness along its length. The lattice fringes of the {100} and {001} planes with a d spacing of 0.38 nm and 0.63 nm, respectively, peculiar to the wurtzite ZnS crystal, can be clearly seen. The growth direction of this tube, for example, is parallel to the [120] crystallographic direction of a ZnS crystal, which is perpendicular to the {100} planes. This is a frequent growth characteristic for materials with the wurtzite (hexagonal close-packed, *hcp*) structure, and has been displayed in many one-dimensional forms with the same structure.^[3f,11] This can be simply explained in terms of a “low-energy” argument; that is, the (1000) plane is one of

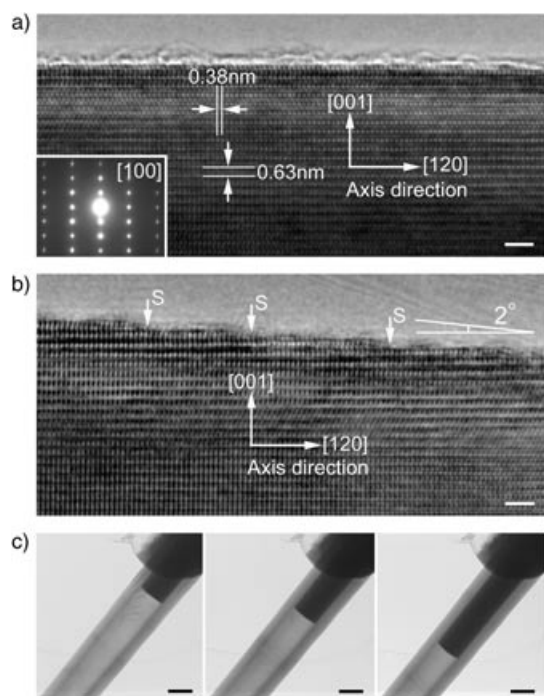


Figure 3. a), b) HRTEM images recorded for the ZnS nanotubes with different wall thicknesses. Scale bars: 2 nm. The lower-left inset in a) shows the corresponding electron diffraction pattern recorded with an incident electron beam along the [100] direction. On the tube surface (shown in b), the atomic steps are marked with "S". c) Consecutive TEM images showing the melting and moving of the Sn-filling in a ZnS nanotube under the slow movement of an electron beam along its length. Scale bars: 100 nm.

the densely arranged planes (it is not the closest stacked plane) in the wurtzite structure, and stacking along [120] thus becomes energetically favorable. As seen from the image, this tube is a structurally uniform single crystal, and no dislocations or other planar defects are observed within it. The edge of the tube is clean and abrupt on an atomic scale, and there are no amorphous layers covering the surface. The corresponding electron diffraction (ED) pattern (the lower-right inset in Figure 3a) can be indexed as the [100] zone axis diffraction pattern of the wurtzite ZnS single crystal. The out-of-focus diffraction pattern also suggests that the long axis or the growth of such a tube occurs along the [120] direction of the ZnS crystal. Careful HRTEM and ED examinations of this tube indicate that the structural uniformity of the single-crystal ZnS tube is maintained throughout the whole length. Figure 3b is an image recorded of a tube whose diameter gradually decreases along its length; it reveals similar imaging characteristics to that of the tube with uniform diameter. In this case, the surface edge is not parallel to the axis of the tube, and a small discrepancy of about 2° is observed with respect to the direction of the tube axis. There are also some atomic steps (marked with "S" on the surface in Figure 3) that are associated with the gradual decrease of the diameter along the length. Research on low melting-point metals confined in carbon nanotubes was pioneered by Ajayan and Iijima,^[12] and since then it has attracted considerable attention.^[13] In the present work, we found that electron-beam irradiation in the

microscope can effectively tailor and adjust the lengths and positions of the Sn-fillings in the ZnS tubes. Figure 3c shows consecutive TEM images recorded on slowly moving an electron beam along the filled tube length; the melting and moving of the Sn-filling within the tube is clearly displayed. A similar phenomenon has been observed previously for encapsulated Sn in carbon nanotubes under electron irradiation.^[14] In the present case, it is possible that an increase in temperature occurs upon irradiating the sample, and that a simultaneous thermal expansion due to a very low basic pressure ($\sim 1 \times 10^{-5}$ Pa) in the TEM chamber favors the movements of the Sn-filling in the ZnS nanotubes.

The present template route for the growth of the Sn-filled ZnS nanotubes was accomplished by combining the decomposition of SnO and the thermal evaporation of ZnS powders. SnO is metastable and will decompose to Sn and SnO₂ at a temperature higher than 300 °C.^[15] Moreover, the higher the reaction temperature, the faster is the rate of the decomposition.^[16] The as-formed Sn may be in the form of small-sized liquid (Sn: m.p. 232 °C^[15]) clusters when reduced from SnO. The Sn clusters are then transported by the carrier gases (N₂) to a lower temperature region in the tube, where they are deposited in the form of a liquid ball on the graphite substrate (Figure 4). The Sn balls provide preferential surface sites for

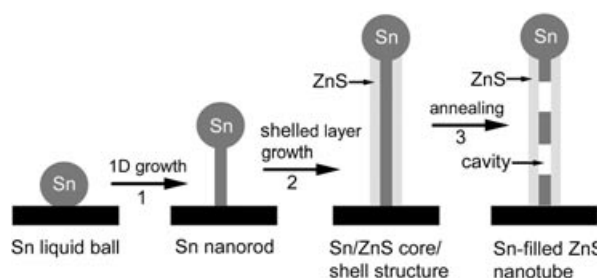


Figure 4. Schematic illustration of the Sn-nanorod-templated process for making single-crystalline ZnS nanotubes. See text for details.

the absorption of the Sn clusters, resulting in the one-dimensional growth of Sn nanorods (Figure 4, step 1). As the processing temperature increases further, the ZnS powders evaporate at a higher rate, producing ZnS vapor. A mono-crystalline ZnS thin layer generated upon condensation of the ZnS vapor grows on the Sn nanorod templates, leading to the formation of the Sn/ZnS core/shell structures (Figure 4, step 2). Annealing for a long period partially evaporates the Sn core out of these structures, or melts and moves the Sn nanorods within the structures, whereas the ZnS shell, which has a high melting point (ZnS: m.p. 1722 °C^[13]) remains intact. As a result, a partially hollow cavity with a ZnS sheath, namely, a single-crystalline ZnS nanotube, is formed (Figure 4, step 3).

Figure 5 shows comparative room-temperature photoluminescence (PL) spectra of the ZnS nanotubes (curve 1) and a commercial ZnS powder (curve 2). The spectrum for the as-grown ZnS nanotubes exhibits a weak and broad (UV) emission band at 335–355 nm and a strong and stable green emission centered at about 528 nm. The band at 335–355 nm corresponds to a band-gap emission of 3.70–3.49 eV. Thus, the

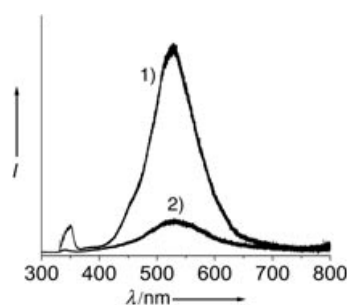


Figure 5. Comparative photoluminescence (PL) spectra of ZnS nanotubes (curve 1) and a commercial ZnS powder (curve 2).

present ZnS nanotubes have a broader energy band gap than that for the bulk material (E_g : ~ 3.65 eV).^[17] The green emission (at ~ 528 nm) for the ZnS nanotubes is nearly seven times higher in intensity than that for the starting commercial ZnS powders. A similar green emission (at ~ 534 nm) has been observed in ZnS nanoribbons.^[34] In this case the emission maybe caused by the presence of some self-activated luminescence centers, probably vacancy states or interstitial states related to the peculiar nanostructures.

In summary, we have synthesized single-crystalline wurtzite-type ZnS nanotubes for the first time by using a simple Sn-nanorod-templated evaporation process. The results suggest that this method might be useful for the synthesis of many other single-crystal nanotubes of the Group II–VI semiconductors.

Experimental Section

The ZnS nanotubes were synthesized in a horizontal high-temperature resistance furnace. A graphite crucible containing a mixture of ZnS (1.5 g) and SnO (0.3 g) (or ZnS (1.5 g), SnO (0.3 g), SnO₂ (0.2 g), and activated carbon (0.1 g)) powders was placed in the central zone of a quartz tube. The furnace was heated to 1150°C at a rate of 10 K min⁻¹, kept at this temperature for 4 h, and then cooled to room temperature. The whole process was carried out under a constant flow of pure N₂ at a rate of 450 mL min⁻¹. The products were collected from the inner wall of the tube and characterized by X-ray diffraction (RINT 2200), scanning electron microscopy (JSM-6700F), and transmission electron microscopy (3000F, equipped with an X-ray energy-dispersive spectrometer (EDS)). The photoluminescence for the as-grown ZnS nanotubes and the starting commercial ZnS powders was measured under the same experimental conditions. The spectra were recorded at room temperature in a spectral range of 300–800 nm using a He–Cd laser line of 325 nm as the excitation source.

Received: March 8, 2004 [Z54205]

Keywords: crystal growth · nanostructures · semiconductors · tin · zinc

[1] S. Iijima, *Nature* **1991**, 354, 56.

[2] See, for example: a) R. Tenne, L. Margulis, M. Genut, G. Hodes, *Nature* **1992**, 360, 444; b) E. J. M. Hamilton, S. E. Dolan, C. M. Mann, H. O. Colijn, C. A. McDonald, S. G. Shore, *Science* **1993**, 260, 659; c) Y. Feldman, E. Wasserman, D. J. Srolovitz, R. Tenne, *Science* **1995**, 267, 222; d) N. G. Chopra, R. J. Luyken, K. Cherrey, V. H. Crespi, M. L. Cohen, S. G. Louie, A. Zettl,

Science **1995**, 269, 966; e) L. Pu, X. M. Bao, J. P. Zou, D. Feng, *Angew. Chem.* **2001**, 113, 1538; *Angew. Chem. Int. Ed.* **2001**, 40, 1490; f) M. Nath, C. N. R. Rao, *Angew. Chem.* **2002**, 114, 3601; *Angew. Chem. Int. Ed.* **2001**, 40, 1490; g) J. H. Jung, H. Kobayashi, K. J. C. van Bommel, S. Shinkai, T. Shimizu, *Chem. Mater.* **2002**, 14, 1445.

- [3] See, for example: a) X. G. Peng, L. Manna, W. D. Yang, J. Wickham, E. Scher, A. Kadavanich, A. P. Alivisatos, *Nature* **2000**, 404, 59; b) O. Wu, N. Zheng, Y. Ding, Y. Li, *Inorg. Chem. Commun.* **2002**, 5, 671; c) C. S. Yang, D. D. Awschalom, G. D. Stucky, *Chem. Mater.* **2002**, 14, 1277; d) Y. W. Wang, G. W. Meng, L. D. Zhang, C. H. Liang, J. Zhang, *Chem. Mater.* **2002**, 14, 1773; e) C. Ma, D. Moore, J. Li, Z. L. Wang, *Adv. Mater.* **2003**, 15, 228; f) Y. Jiang, X. M. Meng, J. Liu, Z. Y. Xie, C. S. Lee, S. T. Lee, *Adv. Mater.* **2003**, 15, 323; g) Y. Jiang, X. M. Meng, J. Liu, Z. R. Hong, C. S. Lee, S. T. Lee, *Adv. Mater.* **2003**, 15, 1195.
- [4] a) B. O. Dabboussi, M. G. Bawendi, O. Onitsuka, M. F. Rubner, *Appl. Phys. Lett.* **1995**, 66, 1316; b) D. L. Klein, R. Roth, A. K. L. Lim, A. P. Alivisatos, P. L. McEuen, *Nature* **1997**, 389, 699; c) H. Weller, *Angew. Chem.* **1998**, 110, 1748; *Angew. Chem. Int. Ed.* **1998**, 37, 1658; d) J. M. Bruchez, M. Moronne, P. Gin, S. Weiss, A. P. Alivisatos, *Science* **1998**, 281, 2013; e) X. F. Duan, Y. Huang, R. Agarwal, C. M. Lieber, *Nature* **2003**, 421, 241.
- [5] C. N. R. Rao, A. Govindaraj, F. L. Deepak, N. A. Gunari, M. Nath, *Appl. Phys. Lett.* **2001**, 78, 1853.
- [6] Y. J. Xiong, Y. Xie, J. Yang, R. Zhang, C. Z. Wu, G. A. Du, *J. Mater. Chem.* **2002**, 12, 3712.
- [7] X. D. Wang, P. X. Gao, J. Li, C. J. Summers, Z. L. Wang, *Adv. Mater.* **2002**, 14, 1732.
- [8] Y. C. Zhu, Y. Bando, Y. Uemura, *Chem. Commun.* **2003**, 836.
- [9] a) C. J. Brumlik, C. R. Martin, *J. Am. Chem. Soc.* **1991**, 113, 3174; b) R. Parthasarathy, C. R. Martin, *Nature* **1994**, 369, 298; c) C. R. Martin, *Science* **1994**, 266, 1961; d) P. M. Ajayan, O. Stephan, P. Redlich, C. Colliex, *Nature* **1995**, 375, 564; e) B. B. Lakshmi, P. K. Dorhout, C. R. Martin, *Chem. Mater.* **1997**, 9, 857; f) J. C. Hulthen, C. R. Martin, *J. Mater. Chem.* **1997**, 7, 1075.
- [10] a) J. Goldberger, R. R. He, Y. F. Zhang, S. Lee, H. Q. Yan, H. -J. Choi, P. D. Yang, *Nature* **2003**, 422, 599; b) J. Q. Hu, Y. Bando, Z. W. Liu, J. H. Zhan, D. Golberg, *Angew. Chem.* **2004**, 113, 65; *Angew. Chem. Int. Ed.* **2004**, 43, 63.
- [11] a) J. Q. Hu, Y. Bando, Z. W. Liu, T. Sekiguchi, D. Golberg, J. H. Zhan, *J. Am. Chem. Soc.* **2003**, 125, 11306; b) Y. Jiang, X. M. Meng, W. C. Yiu, J. Liu, J. X. Ding, C. -S. Lee, S. -T. Lee, *J. Phys. Chem. B* **2004**, 108, 2784; c) K. M. Ip, C. R. Wang, Q. Li, S. K. Harka, *Appl. Phys. Lett.* **2004**, 84, 795; d) Y. C. Zhu, Y. Bando, D. F. Xue, D. Dolberg, *Adv. Mater.* **2004**, 16, 831.
- [12] P. M. Ajayan, S. Iijima, *Nature* **1993**, 361, 333.
- [13] a) Y. Y. Wu, P. D. Yang, *Adv. Mater.* **2001**, 13, 520; b) Y. H. Gao, Y. Bando, *Nature* **2002**, 415, 599; c) Y. B. Li, Y. Bando, D. Golberg, *Adv. Mater.* **2003**, 15, 581.
- [14] W. K. Hsu, M. Terrones, H. Terrones, N. Grobert, A. I. Kirkland, J. P. Hare, K. Prassides, P. D. Townsend, H. W. Kroto, D. R. M. Walton, *Chem. Phys. Lett.* **1998**, 284, 177.
- [15] *Lange's Handbook of Chemistry*, 15th ed. (Ed.: J. A. Dean), McGraw-Hill, New York, **1999**.
- [16] a) D. W. Yuan, R. F. Yan, G. Simkovich, *J. Mater. Sci.* **1999**, 34, 2911; b) J. Q. Hu, X. L. Ma, N. G. Shang, Z. Y. Xie, N. B. Wong, C. S. Lee, S. T. Lee, *J. Phys. Chem. B* **2002**, 106, 3823.
- [17] N. A. Dhas, A. Zaban, A. Gedanken, *Chem. Mater.* **1999**, 11, 806.